Accepted Manuscript

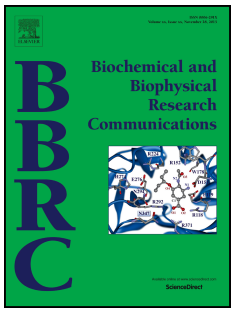

In vitro and *in vivo* inhibition of proangiogenic retinal phenotype by an antisense oligonucleotide downregulating *uPAR* expression

Matteo Lulli, Maurizio Cammalleri, Irene Granucci, Ewa Witort, Federico Di Gesualdo, Antonella Lupia, Rosa Loffredo, Giovanni Casini, Massimo Dal Monte, Sergio Capaccioli

PII: S0006-291X(17)31281-0

DOI: 10.1016/j.bbrc.2017.06.150

Reference: YBBRC 38056

To appear in: *Biochemical and Biophysical Research Communications*

Received Date: 5 June 2017

Accepted Date: 26 June 2017

Please cite this article as: M. Lulli, M. Cammalleri, I. Granucci, E. Witort, F. Di Gesualdo, A. Lupia, R. Loffredo, G. Casini, M. Dal Monte, S. Capaccioli, *In vitro* and *in vivo* inhibition of proangiogenic retinal phenotype by an antisense oligonucleotide downregulating *uPAR* expression, *Biochemical and Biophysical Research Communications* (2017), doi: 10.1016/j.bbrc.2017.06.150.

In vitro and *in vivo* inhibition of proangiogenic retinal phenotype by an antisense oligonucleotide downregulating *uPAR* expression

Matteo Lulli[1*], Maurizio Cammalleri[2], Irene Granucci[1], Ewa Witort[1], Federico Di Gesualdo[1], Antonella Lupia[1], Rosa Loffredo[1], Giovanni Casini[2], Massimo Dal Monte[2#] and Sergio Capaccioli[1#*]

[1]Department of Experimental and Clinical Biomedical Sciences "Mario Serio", University of Florence, viale GB Morgagni 50, 50134 Florence (Italy); [2] Department of Biology, University of Pisa, via San Zeno 31, 56127 Pisa (Italy)

* Corresponding authors. E-mail address: matteo.lulli@unifi.it; sergio.capaccioli@unifi.it

[#] Both authors equally contributed to this paper.

ABSTRACT

Neoangiogenesis is the main pathogenic event involved in a variety of retinal diseases. It has been recently demonstrated that inhibiting the urokinase-type plasminogen activator receptor (uPAR) results in reduced angiogenesis in a mouse model of oxygen-induced retinopathy (OIR), establishing uPAR as a therapeutic target in proliferative retinopathies. Here, we evaluated, in cultured human retinal endothelial cells (HRECs) and in OIR mice, the potential of a specific antisense oligodeoxyribonucleotide (ASO) in blocking the synthesis of uPAR and in providing antiangiogenic effects.

uPAR expression in HRECs was inhibited by lipofection with the phosphorotioated 5'-CGGCGGGTGACCCATGTG-3' ASO-uPAR, complementary to the initial translation site of *uPAR* mRNA. Inhibition of *uPAR* expression via ASO-uPAR was evaluated in HRECs by analyzing VEGF-induced tube formation and migration. In addition, the well-established and reproducible murine OIR model was used to induce retinal neovascularization *in vivo*. OIR mice were injected intraperitoneally with ASO-uPAR and retinopathy was evaluated considering the extent of the avascular area in the central retina and neovascular tuft formation.

The ASO-uPAR specifically decreased *uPAR* mRNA and protein levels in HRECs and mitigated VEGF-induced tube formation and cell migration. Noteworthy, in OIR mice ASO-uPAR administration reduced both the avascular area and the formation of neovascular tufts.

In conclusion, although the extrapolation of these experimental findings to the clinic is not straightforward, ASO-uPAR may be considered a potential therapeutic tool for treatment of proliferative retinal diseases.

Keywords

Human retinal endothelial cells; retinal diseases; VEGF.

INTRODUCTION

Retinal diseases with high social impact are characterized by pathologic vessel proliferation [1, 2]. Generally, pathologic angiogenesis in proliferative retinopathies, including retinopathy of prematurity (ROP), diabetic retinopathy (DR) and age-related macular degeneration (AMD), is triggered by the activation of hypoxia inducible factor-1 (HIF-1), which, in turn, induces more than one hundred genes [3]. Among these HIF-1-induced genes, those coding for vascular endothelial growth factor (VEGF) [2] and urokinase plasminogen activator (uPA) receptor (uPAR) [4, 5] are the most strictly related to retinal angiogenesis.

In particular, there is evidence indicating that the (uPA)/uPAR system is endowed with pleiotropic functions in angiogenesis, which span from extracellular matrix proteolysis to activation of intracellular signaling pathways leading to proliferation and migration of endothelial cells (for two reviews see [4, 5]). So far, VEGF has been considered the master switch of angiogenesis and, therefore, the main therapeutic target for proliferative retinopathies [6-8]. Nevertheless, the uPA/uPAR system appears to play a role that is hierarchically equal [5, 9-11] or even higher [12-14] than that of the VEGF/VEGFR system. This may explain why proliferative retinopathies are associated to overexpression of uPA/uPAR, which appears to be essential for the development of new vessels in the retinas of diabetic mice and rats [10, 15]. This role has been confirmed by findings indicating that uPA/uPAR system inhibition or *uPAR* gene deletion prevent the increase in retinal vessel permeability in rodent models of ROP, DR and AMD, and reduce pathologic angiogenesis in mouse models of ROP and AMD [11, 15-19].

Antisense oligonucleotide (ASO)-based approaches constitute an active area of research aimed to treat human diseases caused by overexpression of a specific protein [20]. ASOs are synthetic nucleic acid segments complementary to and thereby targeting a specific (pre)mRNA [21]. The acquisition that one molecule of mRNA translates a median number of protein reaching nearly 10,000 copies [22], highlights the theoretical advantage of blocking the expression of an overabundant protein by preventing the translation of its mRNA rather than by inhibiting its activity. Up to now, ASOs have demonstrated promising experimental results and are now at different stages of regulatory approval or already approved by the Federal Food and Drug Administration [20, 23].

More than twenty years ago, for the first time we strongly inhibited uPAR expression at the level of its mRNA in cultures of human fibroblasts using a specific ASO (ASO-uPAR) [24]. Having continuously updated our skills on ASO strategies aimed at modulating gene expression in different experimental models [21, 25-27], in the present study we explored the effectiveness of ASO-uPAR in inhibiting angiogenic responses both *in vitro* and *in vivo*. Therefore, we investigated the ASO-

uPAR-induced downregulation of *uPAR* expression and inhibition of the proangiogenic phenotype in cultured human retinal endothelial cells (HRECs) as well as the ability of systemically delivered ASO-uPAR in inhibiting retinal neovascularization in the mouse model of oxygen-induced retinopathy (OIR). The results indicated a high effectiveness of ASO-uPAR in decreasing *uPAR mRNA* and uPAR protein levels in HRECs, in impairing their VEGF-induced proangiogenic phenotype, and in reducing neovascularization in OIR mice. On this basis, we suggest evaluating the antiangiogenic property of ASO-uPAR as a potential therapeutic in proliferative retinopathies.

MATERIAL AND METHODS

Cell culture and ASO transfections.

In vitro studies were performed with HRECs (ACBRI-181, Applied Cell Biology Research Institute, Kirkland, WA). These cells represent a mixture of venous and arterial cell populations. HRECs were cultured in Endothelial Basal Medium-2 (EBM-2; Lonza, USA) supplemented with 10% Fetal Bovine Serum (FBS) and endothelial growth factors (Microvascular Endothelial Cell Growth Medium-2, EGM-2MV SingleQuot, but without addition of gentamicin; Lonza, USA) and grown to 70–80% confluence.

To inhibit *uPAR* expression we used a 5’- 3’-phosphorotioate antisense oligodeoxyribonucleotide (ASO-uPAR) whose sequence was 5’-CGGCGGGTGACCCATGTG-3’(Sigma-Aldrich, St. Louis, MO) [24]. This ASO is complementary to the translational start site of *uPAR* mRNA (residues 224-241 of human *uPAR* mRNA sequence NM_002659.3). A degenerated oligodeoxyribonucleotide (ASO-DEG) sequence with the same phosphorothioate substitutions (5'-NNNNNNNNNNNNNNNNNN-3'; Sigma-Aldrich) was used as a control.

HRECs were transfected with ASO-uPAR or ASO-DEG using Lipofectamine 2000 (Life Technologies, USA). Since it has been previously described that the half-life of ASO-uPAR in the culture medium is about 48 hours [24], cells were treated two times to achieve optimum inhibition of *uPAR* expression. Cells were plated in 6-well culture plates and grown overnight to 70-80% confluence. Cells were then incubated for 3 hours with a mixture of Lipofectamine 2000 and 10 µM of either ASO-uPAR or ASO-DEG. After 48 hours, cells were incubated for 3 hours with a mixture of Lipofectamine 2000 and 5 µM of either ASO-uPAR or ASO-DEG. After 24 hours, cells were subjected to functional assays.

Western-blot analysis.

Western-blot analyses were performed as previously reported [28]. Briefly, cell pellets were lysed with RIPA lysis buffer (50mM Tris (pH 7.4), 150mM NaCl, 1% Triton X-100, 1% sodium deoxycholate, 0.1% SDS, 5mM EDTA) and proteinase inhibitor cocktail (Roche, Mannheim,

Germany). Protein content was quantified by the Bradford method (Bio-Rad, Hercules, CA). The membranes were incubated in a blocking solution consisting of phosphate buffered saline (PBS)/Odyssey Blocking Buffer 1:1 (Lycor Bioscience) for 1 hour at room temperature. They were then incubated overnight at 4°C with rabbit polyclonal anti-uPAR antibody (sc-10815; Santa Cruz Biotechnologies, Santa Cruz, CA) or mouse monoclonal anti-β-actin (A2228; Sigma Aldrich), washed four times with PBS-Tween 0.1% solution, and probed with the secondary goat anti-mouse IRDye® 700CW and goat anti-rabbit IRDye® 800CW antibodies (Li-Cor, USA) according to the manufacturer's instructions. The protein bands were analyzed by the Odyssey Infrared Imaging System (Lycor Bioscience) software for protein quantification.

RNA extraction and quantitative real-time PCR.

Total RNA isolated with the NucleoSpin II Extraction Kit (Macherey-Nagel, Duren, Germany) was quantified with a Q-bit spectrophotometer (Qiagen, Venlo, Netherlands) and visualized by 1.5% PAGE. 500 ng of RNA were then retrotranscribed using ImProm-II reverse transcriptase (Promega, Madison, WI). Quantitative real-time PCR (qPCR) was performed using GoTaq qPCR Master Mix (Promega). The qPCR analysis was carried out in triplicate using the 7500 Fast Real-Time PCR System (Applied Biosystems, Carlsbad, CA). The primers used were Hs-Plaur_1_SG QuantiTect Assay (Qiagen) for *uPAR* and fw: 5'-CGGCTACCACATCCAAGGAA-3' and rv: 5'-GCTGGAATTACCGCGGCT-3' for *18S*. mRNA was quantified with the ΔΔCt method. mRNA levels were normalized to *18S* as an endogenous control.

HREC capillary-like tube formation assay.

Tube formation was assessed as previously described [29]. Growth factor reduced Matrigel was pipetted into pre-chilled 96-well plates and polymerized for 45 min at 37 °C. Transfected HRECs were first starved with EBM-2 containing 0.5% FBS for 18 h and then placed onto the layer of Matrigel ($2x10^4$ cells/well) in 100 µL of EBM-2 containing 0.5% FBS plus 20 ng/mL of VEGF. After 8h incubation, the endothelial cells were photographed using an inverted microscope and the area occupied by tubular-like structures and the tube length were measured using the Angiogenesis Analyzer tool of the ImageJ software (http://imagej.nih.gov.ij/; provided in the public domain by the National Institutes of Health, Bethesda, MD, USA).

Cell Migration assay

Transwells with a pore size of 8.0 µm (Millipore) were inserted into a 24-well plate. Transfected HREC ($5x10^4$ cells/well) were first starved with EBM-2 containing 0.5% FBS for 18 h and then seeded into the upper compartment of the transwells in EBM-2 containing 0.5% FBS. The lower compartment of the chamber was filled with EBM-2 containing 0.5% FBS plus 20ng/ml VEGF. The inserts were incubated at 37°C for 18h and then removed from the plate. Non-migrating

cells on the upper surface of the filters were wiped with a cotton swab, and the filters were fixed and stained with the Diff Quick Kit. Photographs of five random fields per well were taken under an inverted microscope and visible cells were counted.

Murine OIR model and ASO delivery

The well-established and reproducible murine model of hypoxia-induced retinopathy was used to induce retinal neovascularization in mice pups [30]. Experiments were performed on C57BL/6 mice (n = 32), in agreement with the ARVO Statement for the Use of animals in Ophthalmic and Vision Research and in compliance with the Italian guidelines for animal care (DL116/92) and the European Communities Council Directive (86/609/EEC). Mice pups with their nursing mothers were exposed to high oxygen concentration (75±2%) between post-natal day (PD)7 and PD12 in an infant incubator. Oxygen was checked twice daily with an oxygen analyzer (Pro-Custom Elettronica SRL, Milano, Italy). The mice were exposed to room air at PD12, and from PD12 to PD16 they were i.p. injected once a day with 50 mg/kg of either ASO-uPAR (n = 8) or ASO-DEG (n = 8) dissolved in sterile saline (vehicle). As a control, some experimental animals (n = 8) received vehicle. At PD17, mice were anesthetized with Avertin (i.p., 1.2% tribromoethanol and 2.4% amylene hydrate in distilled water, 0.02 mL/g body weight; Sigma-Aldrich, St. Louis, MO) and killed by cervical dislocation. All experiments were performed at the same time of day, to exclude possible circadian influences. The data were collected from both male and female mice and the results combined as there was no apparent gender difference.

Staining of retinal vasculature and quantitative analysis

Dissected retinas were immersion-fixed for 2 hours with 4% paraformaldehyde in 0.1 M phosphate buffer, cryoprotected overnight with 25% sucrose in 0.1 M phosphate buffer and processed for isolectin B4 labeling as whole mounts. Briefly, the retinal whole mounts were freeze-thawed and incubated overnight at 4°C in fluorescein-labeled isolectin B4 (1:200; Vector Laboratories, Burlingmae, CA, USA). The retinas were examined for changes in their vascular pattern with a microscope equipped with epifluorescence (Eclipse Ni-E; Nikon, Amsterdam, The Netherlands). Images of the retinal vasculature were acquired with a digital photocamera (DS-Fi1c camera, Nikon) and processed using an image-editing software (Adobe Photoshop; Adobe Systems, Inc., Mountain View, CA) to create whole retina reconstructions to measure the extent of the avascular area and the total area of preretinal neovascular tufts, according to previous quantification studies [17]. For each experimental condition, quantitative data originated from 8 retinas belonging to 8 different mice.

Statistical analysis

Data are presented as means ± SD of at least three independent experiments. Statistical

significance was evaluated using One-way ANOVA followed by Newman–Keuls' multiple comparison post-test. Differences with $p<0.05$ were considered significant.

RESULTS

ASO-uPAR decreases *uPAR* mRNA and uPAR protein levels in HRECs.

After treatment with ASO-uPAR, *uPAR* mRNA levels were quantified by real-time PCR. A dramatic decrease (about 72%, $p<0.001$) of *uPAR* mRNA levels was observed with ASO-uPAR, while no significant changes were observed in HRECs treated with ASO-DEG used as negative control (Fig 1A). Then, we confirmed that ASO-uPAR effectively downregulates uPAR expression in HRECs by quantifying uPAR protein levels by Western blotting. Figure 1B shows that treatment with ASO-uPAR resulted in a drop of uPAR protein levels of about 65% ($p<0.01$) compared to untreated cells, while treatment with ASO-DEG did not elicit any effect.

ASO-uPAR impairs VEGF-induced tube formation and migration in HRECs.

To shed light on the functional effects of uPAR downregulation obtained with ASO-uPAR treatment, we evaluated if ASO-uPAR impaired the proangiogenic phenotype of HRECs, particularly their ability to form a tubular-like network on Matrigel matrix as well as to migrate through a porous membrane under the angiogenic stimulus elicited by VEGF.

For the first purpose, untreated and ASO-DEG- or ASO-uPAR-treated HRECs were plated on Matrigel matrix and stimulated with VEGF for 12 h. Tube formation was quantified by measuring both the area occupied by tubular-like structures and the tube length. As compared to untreated cells, ASO-DEG did not alter these parameters, while ASO-uPAR significantly reduced the area occupied by tubular like structures (about 60%, $p<0.001$), in good correlation with the reduction in tube length (about 70%, $p<0.001$) (Fig 2A-C).

In order to study the effect of ASO-uPAR treatment on cell migration, untreated and ASO-DEG- or ASO-uPAR-treated HRECs were seeded on a transwell chamber with uncoated filters and cell migration was induced by addition of VEGF in the lower well. Cells detectable on the lower sides of the filters were counted after 24 hours of incubation. ASO-uPAR-treated HRECs were strongly inhibited in their motility: the number of cells crossing the filter was reduced to only about 25% ($p<0.001$) as compared to untreated or ASO-DEG-treated HRECs (Fig 2D, E).

ASO-uPAR reduces neovascularization in OIR mice.

In OIR, the superficial vascular plexus is characterized by a pronounced avascular area without morphologic signs of neovascularization at PD12, followed by neovascular tuft formation starting at PD15 between the central avascular area and the peripheral vascularized retina and reaching its maximal density at PD17.

To disclose the *in vivo* efficacy of ASO-uPAR in inhibiting retinal neovascularization, we used the OIR model and isolectin B4 immunostaining of retinal vessels. Fig 3A-D is representative of the vascular pattern observed at PD17 in retinas of untreated and vehicle-, ASO-DEG- or ASO-uPAR-treated OIR mice. In retinas of untreated mice, a large avascular area was present in the central zone and an excessive regrowth of abnormal superficial vessels leading to preretinal neovascular tufts was observed in the midperipheral retina (Fig. 3A). While vehicle or ASO-DEG treatment did not affect the avascular area or the formation of neovascular tufts (Fig. 3B and C, respectively), the treatment with ASO-uPAR reduced both the extension of the avascular area and the amount of tuft formation (Fig. 3D). Quantitative analysis confirmed these observations. Both the avascular area (Fig 3E) and the neovascular tuft area (Fig 3F) were significantly reduced after ASO-uPAR treatment (about 57%, $p<0.01$, and about 70%, $p<0.001$, respectively).

DISCUSSION

The high worldwide spread of proliferative retinopathies leading to progressive blindness justifies the need for new specific therapies [31-33]. The evidence has recently emerged that, similar to the VEGF/VEGFR system, the uPA/uPAR system is a promising therapeutic target to inhibit retinal neovascularization [5, 9, 11-14, 18]. McGuire et al. achieved a significant inhibition of neovascularization in OIR mice using intraperitoneal injections of a peptide inhibiting the interactions between uPA and uPAR [11]. More recently, another peptide, named UPARANT, which inhibits uPAR activity hindering its interactions with formyl peptide receptors and integrins [34], has been successfully used to reduce retinal and choroidal neovascularization in mouse models of ROP and AMD [16, 17]. In addition, UPARANT has been found to prevent blood retinal barrier breakdown and visual dysfunction in a rat model of DR [19].

Undoubtedly, therapeutic peptides have demonstrated numerous benefits, including high activity per unit mass, high selectivity and specificity, low off-target toxicity, low drug interaction potential and low cost of production. Nonetheless, even higher benefits, mainly in term of potency, may be provided by the ASO strategy. In this respect, we have extensively applied this strategy to inhibit the expression of several genes, also in therapeutic settings [21, 25-27]. In addition, ASOs have been specifically applied for the treatment of eye diseases including cytomegalovirus retinitis, keratitis-induced corneal neovascularization and inherited retinal diseases [35].

Li et al. have clearly shown that a single mRNA molecule may produce a median number of 9,800 protein molecules [22]. Consequently, ASOs may have a clear numerical advantage over peptides since the targets of therapeutic peptides are specific proteins, while those of therapeutic ASOs are specific mRNAs, which are blocked in translation or degraded after ASO targeting. Thus,

the block/degradation of an mRNA molecule could prevent the potential formation of almost 10,000 protein molecules. The main limitation to the use of ASOs as therapeutics lies in the intrinsic characteristics of oligonucleotides, as they are large anionic molecules with relatively scarce bioavailability mainly due to high sensitivity to degradation by endogenous nucleases [36]. In light of this, a great deal of work in the last few years has been concentrated on suitable delivery systems of ASOs and on their protection from nucleases without interfering with their targeting ability. Chemical modifications of oligonucleotide backbone, in particular via phosphorothioation or O-methylation, increase nuclease resistance and binding affinity to mRNA targets, with best results obtained with locked nucleic acids or peptide nucleic acids. On the other hand, coating of ASOs with cationic polymers or complexation of ASOs with cell penetrating peptides or cationic lipids have provided a great improvement in *in vivo* delivery and uptake through plasma membrane [21, 36, 37].

In this study, we demonstrate the effectiveness of an ASO-uPAR in inducing a specific and consistent drop in both *uPAR* mRNA and uPAR protein levels in HRECs. The marked reduction by ASO-UPAR in HREC's ability to form a tubular-like network and to migrate in response to VEGF suggests that uPAR plays a key role as a trigger in the shift towards a proangiogenic phenotype in retinal endothelial cells and is in line with the effects of UPARANT previously observed in HRECs and human umbilical vein endothelial cells [17, 38]. Most importantly, our data demonstrate that ASO-uPAR is highly effective in reducing pathologic angiogenesis *in vivo*. The finding that in OIR mice treated with ASO-uPAR the formation of an avascular area and the neovascularization are almost completely prevented suggests that uPAR may act as a switch between physiological retinal vascular regrowth and neovascularization during the period of relative hypoxia between PD12 and PD17. In this respect, it should be noted that in OIR mice peptide inhibitors of the uPA/uPAR system have been shown to reduce neovessel growth without affecting the central avascular area [11, 17], indicating that inhibiting uPAR stimulation is sufficient to counteract angiogenic processes but cannot stimulate physiological intraretinal revascularization. The most obvious explanation is that this difference in the effects of uPAR peptide inhibitors and ASO-uPAR might reside in the fact that the first interfere with uPAR signaling, while the last inhibits uPAR expression. However, at present there are no sufficient data available for further speculations, and this issue will be addressed in future studies.

Taken together, the results presented here not only confirm that the uPA/uPAR system, belonging to a molecular circuit involving VEGF and other growth factors [39], plays a key role in the VEGF-induced proangiogenic phenotype both *in vitro* and *in vivo*, but also demonstrate that this phenotype can be successfully inhibited with an ASO approach. Because of the limited efficacy of

anti-VEGF therapies for proliferative retinopathies, the exploitation of new effective strategies is a major challenge in ophthalmology. Although further studies will be needed to evaluate the translational impact of our current results, for the first time we present ASO-uPAR as a candidate therapeutic tool for treating proliferative retinopathies.

Acknowledgements

This work was supported by the Italian Space Agency (ASI).

FIGURE LEGENDS

Figure 1 – Effects of ASO-uPAR transfection on *uPAR* expression in HRECs. **A**) Levels of *uPAR* mRNA were evaluated by qPCR. Data were analyzed by the ΔΔCt method using *18S* RNA as the internal standard. **B**) Levels of uPAR protein were evaluated by Western-blot and Odyssey Infrared Imaging System analysis. Protein expression was relative to the loading control β-actin. Data are the mean ± SD (n = 3). *p<0.001; **p<0.01 vs untreated.

Figure 2 – Effect of ASO-uPAR transfection on VEGF-induced tube formation and migration of HRECs. **A**) Representative fields of tube-forming HRECs as seen in light microscopy. Endothelial tube formation was evaluated and quantified as the area occupied by tubular-like structures (**B**) and tube length (**C**). **D**) Light microscopy images showing Diff Quick stained cells that have migrated on the bottom side of transwell membranes with a pore size of 8.0 µm. Migration was quantitated in triplicate membranes by counting the cells in five different fields of each membrane (**E**). Data are the mean ± SD (n = 3). *p<0.001 vs untreated.

Figure 3 – Effect of ASO-uPAR in OIR mice. A-D) Representative images of retinal whole-mounts, from mice untreated (**A**) or treated with vehicle (**B**), ASO-DEG (**C**) or ASO-uPAR (**D**) stained with fluorescein labeled isolectin B4. The extent of the avascular area (**E**) and the tuft area (**F**) were quantitatively evaluated. Data are the mean ± SD (n = 8). *p<0.01 and **p<0.001 vs untreated. Scale bar, 1mm.

REFERENCES

[1] P. Sapieha, D. Hamel, Z. Shao, J.C. Rivera, K. Zaniolo, J.S. Joyal, et al., Proliferative retinopathies: angiogenesis that blinds, Int. J. Biochem. Cell Biol. 42 (2010) 5-12.

[2] P.A. Campochiaro, Molecular pathogenesis of retinal and choroidal vascular diseases, Prog. Retin. Eye Res. 49 (2015) 67-81.

[3] G.L. Semenza, Hypoxia-inducible factors in physiology and medicine, Cell 148 (2012) 399-408.

[4] A. Laurenzana, G. Fibbi, F. Margheri, A. Biagioni, C. Luciani, M. Del Rosso, et al., Endothelial Progenitor Cells in Sprouting Angiogenesis: Proteases Pave the Way, Curr. Mol. Med. 15 (2015) 606-620.

[5] J.M. Breuss, P. Uhrin, VEGF-initiated angiogenesis and the uPA/uPAR system, Cell Adh. Migr. 6 (2012) 535-615.

[6] R. Simo, C. Hernandez, Intravitreous anti-VEGF for diabetic retinopathy: hopes and fears for a new therapeutic strategy, Diabetologia 51 (2008) 1574-1580.

[7] M.S. Tolentino, A.J. Tolentino, M.J. Tolentino, Current and investigational drugs for the treatment of diabetic retinopathy, Expert Opin. Investig. Drugs. 25 (2016) 1011-1022.

[8] L. Eldweik, I.S. Mantagos, Role of VEGF Inhibition in the Treatment of Retinopathy of Prematurity, Semin. Ophthalmol. 31 (2016) 163-168.

[9] E.S. Colombo, G. Menicucci, P.G. McGuire, A. Das, Hepatocyte growth factor/scatter factor promotes retinal angiogenesis through increased urokinase expression, Invest. Ophthalmol. Vis. Sci. 48 (2007) 1793-1800.

[10] A.B. El-Remessy, M.A. Behzadian, G. Abou-Mohamed, T. Franklin, R.W. Caldwell, R.B. Caldwell, Experimental diabetes causes breakdown of the blood-retina barrier by a mechanism involving tyrosine nitration and increases in expression of vascular endothelial growth factor and urokinase plasminogen activator receptor, Am. J. Pathol. 162 (2003) 1995-2004.

[11] P.G. McGuire, T.R. Jones, N. Talarico, E. Warren, A. Das, The urokinase/urokinase receptor system in retinal neovascularization: inhibition by A6 suggests a new therapeutic target, Invest. Ophthalmol. Vis. Sci. 44 (2003) 2736-2742.

[12] R.A. Alexander, G.W. Prager, J. Mihaly-Bison, P. Uhrin, S. Sunzenauer, B.R. Binder, et al., VEGF-induced endothelial cell migration requires urokinase receptor (uPAR)-dependent integrin redistribution, Cardiovasc. Res. 94 (2012) 125-135.

[13] G.W. Prager, J.M. Breuss, S. Steurer, D. Olcaydu, J. Mihaly, P.M. Brunner, et al., Vascular endothelial growth factor receptor-2-induced initial endothelial cell migration depends on the presence of the urokinase receptor, Circ. Res. 94 (2004) 1562-1570.

[14] V. Stepanova, P.S. Jayaraman, S.V. Zaitsev, T. Lebedeva, K. Bdeir, R. Kershaw R, et al., Urokinase-type Plasminogen Activator (uPA) Promotes Angiogenesis by Attenuating Proline-rich Homeodomain Protein (PRH) Transcription Factor Activity and De-repressing Vascular Endothelial Growth Factor (VEGF) Receptor Expression, J. Biol. Chem. 291 (2016) 15029-15045.

[15] A.B. El-Remessy, T. Franklin, N. Ghaley, J. Yang, M.W. Brands, R.B. Caldwell, et al., Diabetes-induced superoxide anion and breakdown of the blood-retinal barrier: role of the VEGF/uPAR pathway, PLoS One 8 (2013) e71868.

[16] M. Cammalleri, M. Dal Monte, F. Locri, L. Lista, M. Aronsson, A. Kvanta, et al., The Urokinase Receptor-Derived Peptide UPARANT Mitigates Angiogenesis in a Mouse Model of Laser-Induced Choroidal Neovascularization, Invest. Ophthalmol. Vis. Sci. 57 (2016) 2586-2597.

[17] M. Dal Monte, S. Rezzola, M. Cammalleri, M. Belleri, F. Locri, L. Morbidelli, et al., Antiangiogenic Effectiveness of the Urokinase Receptor-Derived Peptide UPARANT in a Model of Oxygen-Induced Retinopathy, Invest. Ophthalmol. Vis. Sci. 56 (2015) 2392-2407.

[18] L. Le Gat, K. Gogat, C. Bouquet, M. Saint-Geniez, D. Darland, L. Van Den Berghe, et al., In vivo adenovirus-mediated delivery of a uPA/uPAR antagonist reduces retinal neovascularization in a mouse model of retinopathy, Gene Ther. 10 (2003) 2098-2103.

[19] M. Cammalleri, F. Locri, S. Marsili, M. Dal Monte, C. Pisano, L.L. Mancinelli, et al., The Urokinase Receptor-Derived Peptide UPARANT Recovers Dysfunctional Electroretinogram and Blood-Retinal Barrier leakage in a Rat Model of Diabetes. Invest. Ophthalmol. Vis. Sci. 2017 *in press*.

[20] X. Chi, P. Gatti, T. Papoian, Safety of antisense oligonucleotide and siRNA-based therapeutics, Drug Discov. Today. 22 (2017) 823-833.

[21] N. Schiavone, M. Donnini, A. Nicolin, S. Capaccioli, Antisense oligonucleotide drug design, Curr. Pharm. Des. 10 (2004) 769-784.

[22] J.J. Li, P.J. Bickel, M.D. Biggin, System wide analyses have underestimated protein abundances and the importance of transcription in mammals, PeerJ. 2 (2014) e270.

[23] C.A. Stein, D. Castanotto, FDA-Approved Oligonucleotide Therapies in 2017, Mol. Ther. 25 (2017) 1069-1075.

[24] A. Quattrone, G. Fibbi, E. Anichini, M. Pucci, A. Zamperini, S. Capaccioli, et al., Reversion of the invasive phenotype of transformed human fibroblasts by anti-messenger oligonucleotide inhibition of urokinase receptor gene expression, Cancer Res. 55 (1995) 90-95.

[25] L. Papucci, E. Witort, AM. Bevilacqua, M. Donnini, M. Lulli, E. Borchi, et al., Impact of targeting the adenine- and uracil-rich element of bcl-2 mRNA with oligoribonucleotides on apoptosis, cell cycle, and neuronal differentiation in SHSY-5Y cells, Molecular Pharmacology 73 (2008) 498-508.

[26] E. Witort, M. Lulli, V. Carloni, S. Capaccioli, Anticancer activity of an antisense oligonucleotide targeting TRADD combined with proteasome inhibitors in chemoresistant hepatocellular carcinoma cells, Journal of Chemotherapy 25 (2013) 292-297.

[27] F. Di Gesualdo, S. Capaccioli, M. Lulli, A pathophysiological view of the long non-coding RNA world, Oncotarget 5 (2014) 10976-10996.

[28] A. Lupia, S. Peppicelli, E. Witort, F. Bianchini, V. Carloni, N. Pimpinelli, et al., CD63 tetraspanin is a negative driver of epithelial-to-mesenchymal transition in human melanoma cells, J. Invest. Dermatol. 134 (2014) 2947-2956.

[29] M. Lulli, M. Cammalleri, I. Fornaciari, G. Casini, M. Dal Monte, Acetyl-11-keto-?-boswellic acid reduces retinal angiogenesis in a mouse model of oxygen-induced retinopathy, Experimental Eye Research 135 (2015) 67-80.

[30] L.E. Smith, E. Wesolowski, A. McLellan, S.K. Kostyk, R. D'Amato, R. Sullivan R, et al., Oxygen-induced retinopathy in the mouse, Invest. Ophthalmol. Vis. Sci. 35 (1994) 101-111.

[31] P. Hahn, K. Acquah, S.W. Cousins, P.P. Lee, F.A. Sloan, Ten-year incidence of age-related macular degeneration according to diabetic retinopathy classification among medicare beneficiaries, Retina 33 (2013) 911-919.

[32] R.L. Thomas, F. Dunstan, S.D. Luzio, S. Roy Chowdury, S.L. Hale, R.V. North, et al., Incidence of diabetic retinopathy in people with type 2 diabetes mellitus attending the Diabetic Retinopathy Screening Service for Wales: retrospective analysis, Bmj. 344 (2012) e874.

[33] R. Klein, C.E. Myers, K.E. Lee, B.E. Klein, 15-year cumulative incidence and associated risk factors for retinopathy in nondiabetic persons, Arch. Ophthalmol. 128 (2010) 1568-1575.

[34] M.V. Carriero, K. Bifulco, M. Minopoli, L. Lista, O. Maglio, L. Mele, et al., UPARANT: a urokinase receptor-derived peptide inhibitor of VEGF-driven angiogenesis with enhanced stability and in vitro and in vivo potency, Mol. Cancer. Ther. 15 (2014) 1092-1104.

[35] R.W. Collin, A. Garanto, Applications of antisense oligonucleotides for the treatment of inherited retinal diseases, Curr. Opin. Ophthalmol. 28 (2017) 260-266.

[36] M. Gooding, M. Malhotra, J.C. Evans, R. Darcy, C.M. O'Driscoll, Oligonucleotide conjugates - Candidates for gene silencing therapeutics, Eur. J. Pharm. Biopharm. 107 (2016) 321-340.

[37] P. Jolly, P. Estrela, M. Ladomery, Oligonucleotide-based systems: DNA, microRNAs, DNA/RNA aptamers, Essays Biochem. 60 (2016) 27-35.

[38] C. Motta, G. Lupo, D. Rusciano, M. Olivieri, L. Lista, M. De Rosa, et al., Molecular Mechanisms Mediating Antiangiogenic Action of the Urokinase Receptor-Derived Peptide UPARANT in Human Retinal Endothelial Cells, Invest. Ophthalmol. Vis Sci. 57 (2016) 5723-5735.

[39] M. Poettler, M. Unseld, J. Mihaly-Bison, P. Uhrin, F. Koban, B.R. Binder et al., The urokinase receptor (CD87) represents a central mediator of growth factor-induced endothelial cell migration, Thromb. Haemost. 108 (2012) 357-366.

Figure 1

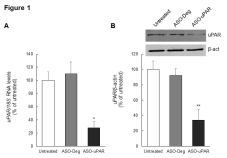

Figure 2

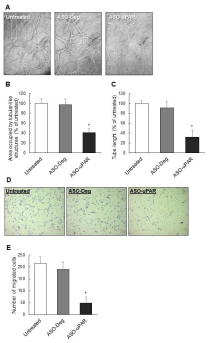

Figure 3